



RESEARCH ARTICLE

Quantitative detections of TP53 gene mutations improve the diagnosis and prognostic prediction of biliary tract cancers using droplet digital PCR

Xiao Xiao^{1,2}  | Jun Zhou² | Meng Fang² | Jun Ji² | Chenjun Huang² | Fei Du² | Wenchao Ai² | Ying Wang² | Zhiyuang Gao¹ | Zhiquan Qiu² | Chunfang Gao^{1,2} 

¹Clinical Laboratory Medicine Center, Yueyang Hospital of Integrated Traditional Chinese and Western Medicine, Shanghai University of Traditional Chinese Medicine, Shanghai, China

²Department of Laboratory Medicine, Shanghai Eastern Hepatobiliary Surgery Hospital, Shanghai, China

Correspondence

Chunfang Gao, Clinical Laboratory Medicine Center, Yueyang Hospital of Integrated Traditional Chinese and Western Medicine, Shanghai University of Traditional Chinese Medicine, 110 Ganhe Road, Shanghai, 200437, P.R. China. Department of Laboratory Medicine, Shanghai Eastern Hepatobiliary Surgery Hospital, 225 Changhai Road, Shanghai, 200438, China. Email: gaocf1115@163.com

Funding information

The Innovation Group Project of Shanghai Municipal Health Commission [2019CXJQ03]

Abstract

Objective: Biliary tract cancer (BTC) is a rare malignancy and lack of effective diagnostic and prognostic marker. Here, we aimed to investigate the clinical implication of TP53 mutation detection in BTC using droplet digital PCR (ddPCR).

Methods: TP53 gene (loci p.R175H, p.R248Q, p.R248W, and p.R273H) mutation frequencies of 45 pairs of tumor tissues (TTs) and adjacent normal tissues (ANTTs) were analyzed, respectively, using ddPCR. Meanwhile, the same detections were conducted in plasma cell-free DNA (cfDNA) of 156 subjects including BTC, disease control (DC), and healthy controls (HC). The logistic regression algorithm was established to identify BTC. The correlations between mutations and clinicopathological features as well as the effects of TP53 mutation frequency on BTC prognosis were assessed.

Results: The higher mutation of p.R175H was found in TTs compared with ANTT ($p = 0.006$). The mutation at p.R273H in cfDNA was also higher in BTC when compared with DC and HC ($p < 0.05$). The logistic algorithms combining p.R273H mutation demonstrated the higher diagnostic efficacy trend than carbohydrate antigen 19-9 (CA19-9), carcinoembryonic antigen (CEA), and alpha-fetoprotein (AFP) in identifying BTC from DC (the area under the curves of the algorithm: 0.845, 95% CI:0.775–0.914). The median overall survival (OS) and progression-free survival (PFS) were significantly shorter when the BTC patients harboring the p.R273H mutation (OS: $p = 0.032$; PFS: $p = 0.046$).

Conclusion: This study revealed for the first time that the quantitative TP53 mutations using the ddPCR might serve as a potential genetic biomarker for BTC diagnosis and prognosis assessment.

KEYWORDS

biliary tract cancers, diagnosis, droplet digital PCR, p.R273H, prognosis, TP53

Xiao Xiao and Jun Zhou have contributed equally to this work.

This is an open access article under the terms of the Creative Commons Attribution-NonCommercial-NoDerivs License, which permits use and distribution in any medium, provided the original work is properly cited, the use is non-commercial and no modifications or adaptations are made.

© 2021 The Authors. *Journal of Clinical Laboratory Analysis* published by Wiley Periodicals LLC.

1 | INTRODUCTION

Biliary tract cancer (BTC) is anatomically classified as gallbladder carcinoma (GBC), cholangiocarcinoma (CCA), and the ampullary carcinoma. Cholangiocarcinoma includes extrahepatic cholangiocarcinoma (ECC) and intrahepatic cholangiocarcinoma (ICC).¹ Although the incidence rate of BTC is relatively low, BTC is characterized by early lymph node and distant metastases and, therefore, often diagnosed lately when the diseases are already in advanced stages.² Up to now, tumor resection is still the main therapeutic option although only a small percentage of patients are eligible and curate without recurrence.³ BTC is a heterogeneous group of related but distinct diseases with various clinical features and different genetics changes.⁴ Characterizations of BTC at the genetic levels are essential for understanding its pathogenesis before exploring new diagnostic and therapeutic options for personalized medicine.⁵ Molecular typing of BTC will be promising for early identification and prognosis assessment improving patients' outcome.⁶

Molecular diagnostic technology has now been proved to be an important and even essential method for targeted therapy and immunotherapy for precision oncology.⁷ The clinical application of molecular detection has become more and more feasible due to the progress of new technology during recent half a century.⁸ In particular, digital PCR (dPCR) and next-generation sequencing (NGS) are typical important technologies for liquid biopsy which includes detection of circulating tumor cells (CTCs), circulating tumor DNA (ctDNA), and exosomes in cancer patients.^{9,10} Quantitative real-time PCR (qPCR), one of the method of choice for molecular diagnostics, is fundamental in preclinical and clinical research.¹¹ Recently, the development of dPCR represents an innovative evolution of qPCR that may outperform qPCR in clinical applications.¹² Unlike qPCR, dPCR does not rely on calibration curves for absolute quantification of a DNA target molecule.¹³⁻¹⁵ In addition, dPCR has further exhibited a number of unique advantages over qPCR, including decreased variability and superior sensitivity (<0.1%).¹⁶

The tumor suppressor gene tumor protein p53 (TP53) is one of the most commonly mutated genes in various malignancies.¹⁷ Mutations in TP53 not only disrupt its tumor suppressor function, but also are associated with a worsened prognosis and cause resistance to cancer therapy.^{17,18} In our previous study, we found that the genetic abnormality of TP53 occurred as high as 51.7% in the CCA in a 450 cancer panel exploration using NGS.¹⁹ Meanwhile, our study using the case results from the catalog of somatic mutations in cancer (COSMIC) database (<https://cancer.sanger.ac.uk/cosmic>) indicated that p.R175H, p.R248Q, p.R248W, and p.R273H were the most four common mutations of TP53 in BTC. Whether the quantitative mutation frequencies of p.R175H, p.R248Q, p.R248W, and p.R273H indicating the detailed genomic characteristics of TP53 gene contribute to the diagnosis and prognosis evaluation of BTC remains unknown.

Therefore, in this study, we conducted a retrospective case-control study assessing the clinical implications of quantitative TP53 mutations using the droplet-based dPCR in both tissue and

cell-free DNA (cfDNA) in BTC patients aiming to identify the potential genetic biomarkers for BTC diagnosis and prognosis assessment.

2 | MATERIALS AND METHODS

2.1 | Study design and participants

Totally the 201 subjects with BTC (including GBC, ECC, and ICC) who underwent radical surgical resection and the study controls [including calculous cholecystitis as disease control (DC) and healthy control (HC)] from Shanghai Eastern Hepatobiliary Surgery Hospital (EHBH, Shanghai, China) were recruited into this study from January 2014 to December 2019 (Figure 1). The study protocol was approved by Institutional Ethics Committee of Shanghai Eastern Hepatobiliary Surgery Hospital (EHBH KY2020-02-012). Informed consent was obtained from all subjects, and the data were analyzed anonymously.

Entry criteria of BTC patients included: (1) being diagnosed as BTC by histology; (2) no other associated malignancies or probable metastatic biliary tract tumor; and (3) no other anticancer treatment. Exclusion criteria were subjects with (1) incomplete medical data; (2) mixed-type BTC; and (3) no blood or tissue sample available.

Calculous cholecystitis as disease control (DCs) in this study was diagnosed when the following criteria is met: (1) clinical manifestations and (2) being diagnosed as calculous cholecystitis by B-ultrasound and X-ray cholecystography. The exclusion criteria were: (1) a history of chronic diseases, such as diabetes and coronary heart disease and (2) gender and age mismatch with BTC. Healthy controls (HCs) were demographic healthy blood donors with routine biochemical tests, no history of biliary diseases, and any malignancies.

2.2 | Sample and data collection

Peripheral blood specimens were collected at the time of diagnosis before treatment. Meanwhile, tissue specimens [tumor tissue (TT) and adjacent normal tissue (ANTT)] were obtained during the operation. For all subjects, specimens were stored at -80°C until analysis.

Relevant demographic and clinical data including patients' age, gender, and pathological results were recorded. All laboratory tests, such as immunological detections of carbohydrate antigen 199 (CA19-9), carcinoembryonic antigen (CEA), and alpha-fetoprotein (AFP) as well as biochemical parameters of liver function, were conducted before surgeries. Biochemical tests were conducted using standard methods and matched reagents on 7600 Analyzer (Hitachi, Tokyo, Japan). Immunological detections were determined on a E170 modular with matched reagents (Roche, Basel, Switzerland). The cutoff value for CA19-9 was 39.0 U/ml, CEA 10.0 ug/L, AFP 20.0 ug/L, and total bile acids (TBA) 12.0 umol/L, as recommended by the manufacturers and the relevant clinical practice guideline.

Histopathological studies of the resected specimens, including tumor diameter and the tumor number, capsule integrity, nodule

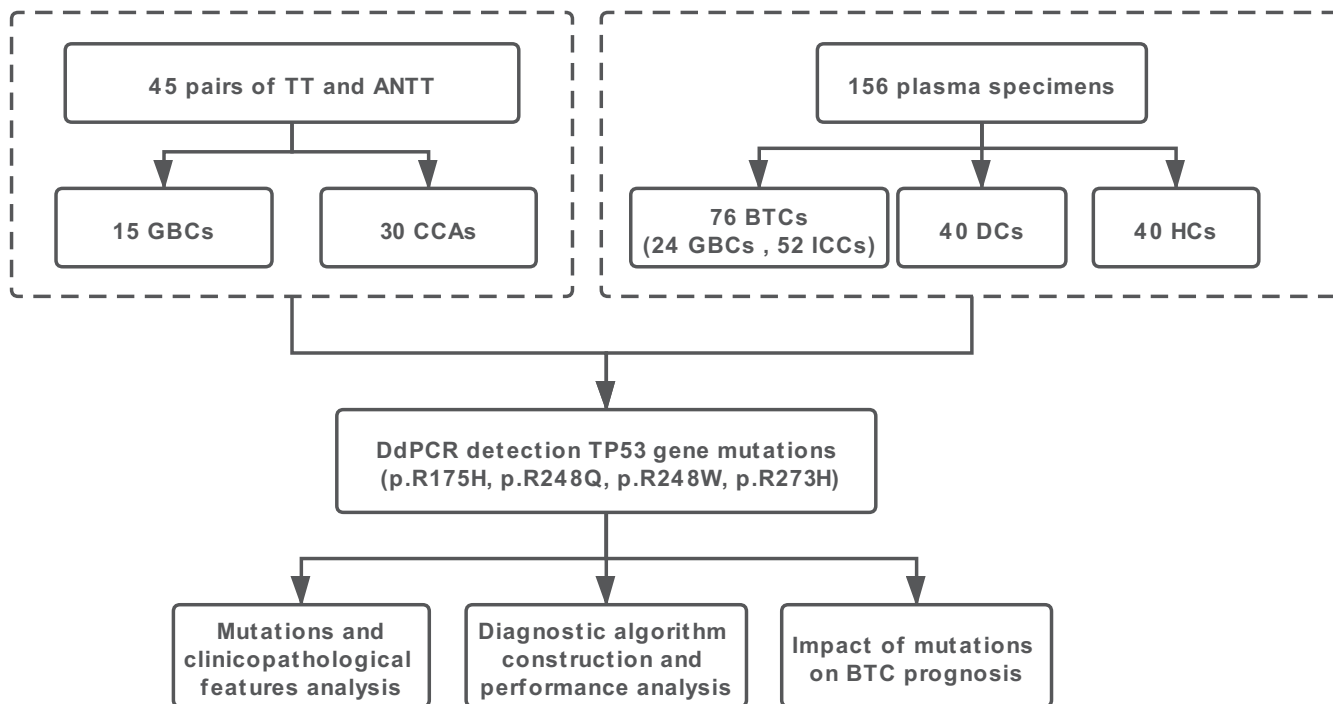


FIGURE 1 Study design and flowchart. Totally the 201 subjects with BTC (including GBC and CCA) and study control (including DC and HC) who met the inclusion criteria were enrolled. The 45 pairs of TT and ANTT were obtained during the operation. The 156 plasma specimens were collected at the time of diagnosis before treatment. The ddPCR was used to detect the four loci of TP53 gene mutations for both the tissue DNA and plasma-cfDNA. The correlations between TP53 mutations and clinicopathological features as well as the impact of mutation on prognosis were assessed. BTC, biliary tract cancer; GBC, gallbladder cancer; CCA, cholangiocarcinoma; ICC, intrahepatic cholangiocarcinoma; TT, tumor tissue; ANTT, adjacent non-tumor tissue; DC, disease control group; and HC, healthy control group

metastasis, and the TNM staging, were completed independently by two experienced pathologists.

The enrolled patients were followed up every 3 months during the first 2 years after surgery and then every 3–6 months thereafter until cancer-induced death or dropout from our project. Progression-free survival (PFS) was measured from the first day of treatment to the date of first objective or clinical sign, death (whichever came first) or to the date of last follow-up visit for patients censored without progression. Overall survival (OS) was measured from the first day of treatment to the date of death or the last date of the follow-up program.

2.3 | Tissue DNA/plasma cfDNA extraction and droplet dPCR detection

CfDNA was extracted from plasma with an average volume of 600 μ L using the MagMAXTM cell-free DNA isolation kit (Thermo Fisher). For tissue DNA extraction, a tissue nucleic acid extraction kit (Ningbo Youcheng Biological Pharmaceutical Co. Ltd.) was used according to the manufacturer's instruction.

Droplet dPCR (ddPCR) was performed on the Bio-Rad QX200 according to the manufacturer's instruction (Bio-Rad). Primers and Taqman probe pairs of four loci of TP53 gene (p.R175H, p.R248Q, p.R248W, and p.R273H) were custom-designed (Shanghai Gemple

Biotech Co. Ltd.). Briefly, 900 nM probes and 250 nM primers were mixed with 2 \times Droplet PCR Supermix (Bio-Rad, Hercules, USA), 5 μ l of template DNA, and H₂O to become 20 μ l for each reaction. The reaction mixture was placed into the sample well of the DG8 cartridge (Bio-Rad, Hercules, USA). A volume of 70 μ l of droplet generation oil was loaded into the oil well, and droplets were formed in the droplet generator (Bio-Rad). After processing, the droplets were transferred to a 96-well PCR plate (Eppendorf). The PCR amplification was carried out on Veriti (Thermo Fisher) with the following thermal profile: hold at 95°C for 10 min, 40 cycles of 94°C for 30 s and 52°C (p.R175H) / 60°C (p.R248Q) / 60°C (p.R248W) / 55°C (p.R273H) for 1 min (ramp 2°C/s), 1 cycle at 98°C for 10 min, and ending at 4°C. After amplification, the plate was loaded on the QX 200 droplet reader (Bio-Rad), and the droplets from each well of the plate were read automatically. QuantaSoft software v.1.5 (Bio-Rad) was used to count the PCR-positive and PCR-negative droplets to provide absolute quantification of the target DNA. The cutoff value for p.R175H was 0.10%, p.R248Q 0.20%, p.R248W 0.10%, and p.R273H 0.05%, as recommended by the kit manufacturer (Shanghai Gemple Biotech Co. Ltd.).

TP53 p.R175H/p.R273H reference standard (Cobioer Biosciences Co. Ltd.) was used for the accuracy assessment for our ddPCR detection system. The allelic frequency of standard was 100%; we diluted it into 50.00%, 10.00%, 1.00%, and 0.10% with dH₂O as templates and detected using this ddPCR system, respectively.

2.4 | Statistical analysis

All statistical analysis and scientific graphics in this study were performed in SPSS 21.0 (IBM) and GraphPad Prism 8.0 (GraphPad Software). The stratified analysis was performed according to the diameter, number of tumors, and TNM stages in BTC group. For categorical variables, the chi-squared test or Fisher's exact test was performed to calculate the difference of rate in different cohorts. Mutation frequencies between TT and ANTT were analyzed using the χ^2 test. Step-wise logistic regression was used to construct diagnostic algorithm models. Receiver operating characteristic (ROC) curves were applied to evaluate the efficacies of diagnostic models in discriminating BTC from control groups. The area under curve (AUC) and its 95% confidence interval (CI) were calculated. PFS and OS analyses were conducted with the Kaplan-Meier method and log-rank test. The p value <0.05 was defined as statistically significant.

3 | RESULTS

3.1 | Quantitative TP53 mutation detection in tissues and the comparison between TT and ANTT

The clinical characteristics, serum laboratory indexes, and TNM stages of 45 cases of BTC with TTs and matched ANTTs are shown in Table S1. The mutation frequencies of p.R175H, p.R248Q, p.R248W, and p.R273H in TP53 genes showed no significant differences between TTs and ANTTs, with the exception of p.R175H. Higher mutation of p.R175H ($p = 0.006$) occurred in TTs (Figure 2).

3.2 | Quantitative TP53 mutation detection in plasma cfDNA and its correlation with clinical pathological features

The demographic and clinical information of 156 enrolled subjects including two subgroups of BTC (GBC and ICC) and two subgroups of control (DC and HC) for cfDNA detection are shown in Table S2. The CA19-9, AFP, CEA, and TBA showed significant differences between BTC and the control group ($p < 0.05$). The mutation frequencies of loci p.R175H, p.R248Q, p.R248W, and p.R273H of TP53 gene from plasma cfDNA are presented in Figure 3. We found that the mutations at p.R175H and p.R273H were much higher in GBC/BTC compared with TCs ($p < 0.05$). Meanwhile, the mutation frequencies in ICCs at p.R273H were also higher than that in TC ($p < 0.05$). In addition, patients harboring the p.R273H mutation had more tumor numbers compared with those without the mutation ($p = 0.005$, Table 1). No significant differences in tumor diameter and TNM stage were found between the patients with or without the mutations at p.R175H, p.R248Q, p.R248W, and p.R273H ($p > 0.05$, Table 1).

3.3 | Logistic regression model construction and diagnostic efficacy assessment based on TP53 mutations

Since among the four loci of TP53, p.R273H was demonstrated as the most significant factors for discrimination BTC and controls (see Figure 3), we then constructed the logistic algorithms combining p.R273H mutation and the routine laboratory tests based on step-wise logistic regression. Firstly, Model273-1 ($=0.431 \times p.R273H + 0.482 \times AFP + 0.005 \times CA19-9 - 1.557$) was developed for discriminating BTC from DC (calculous cholecystitis). As shown in Figure 4A and Table 2, Model273-1 showed the best trend with AUC as high as 0.845 (95% CI: 0.775–0.914) compared with CA19-9 (AUC = 0.786, 95% CI: 0.704–0.867), CEA (AUC = 0.751, 95% CI: 0.657–0.845), and AFP (AUC = 0.692, 95% CI: 0.596–0.788). For identifying another different types of BTC, Model273-2 ($=0.433 \times p.R273H + 0.005 \times CA19-9 - 1.756$) was constructed for differentiating GBC from DC. The AUC of Model273-2 (AUC = 0.908, 95% CI: 0.831–0.985) also showed a better diagnostic efficacy than CA19-9 (AUC = 0.810, 95% CI: 0.691–0.929), CEA (AUC = 0.799, 95% CI: 0.679–0.919), and AFP (AUC = 0.689, 95% CI: 0.553–0.825) (Figure 4B, Table 2). Furthermore, Model273-3 ($=0.912 \times p.R248W + 0.411 \times p.R273H + 0.573 \times AFP + 0.005 \times CA19-9 - 2.156$) was constructed for distinguishing ICC from DC, still the AUC of Model273-3 (AUC = 0.844, 95% CI: 0.764–0.924) was much better than that of CA19-9 (AUC = 0.775, 95% CI: 0.679–0.870), CEA (AUC = 0.729, 95% CI: 0.623–0.836), and AFP (AUC = 0.694, 95% CI: 0.587–0.801) respectively (Figure 4C, Table 2).

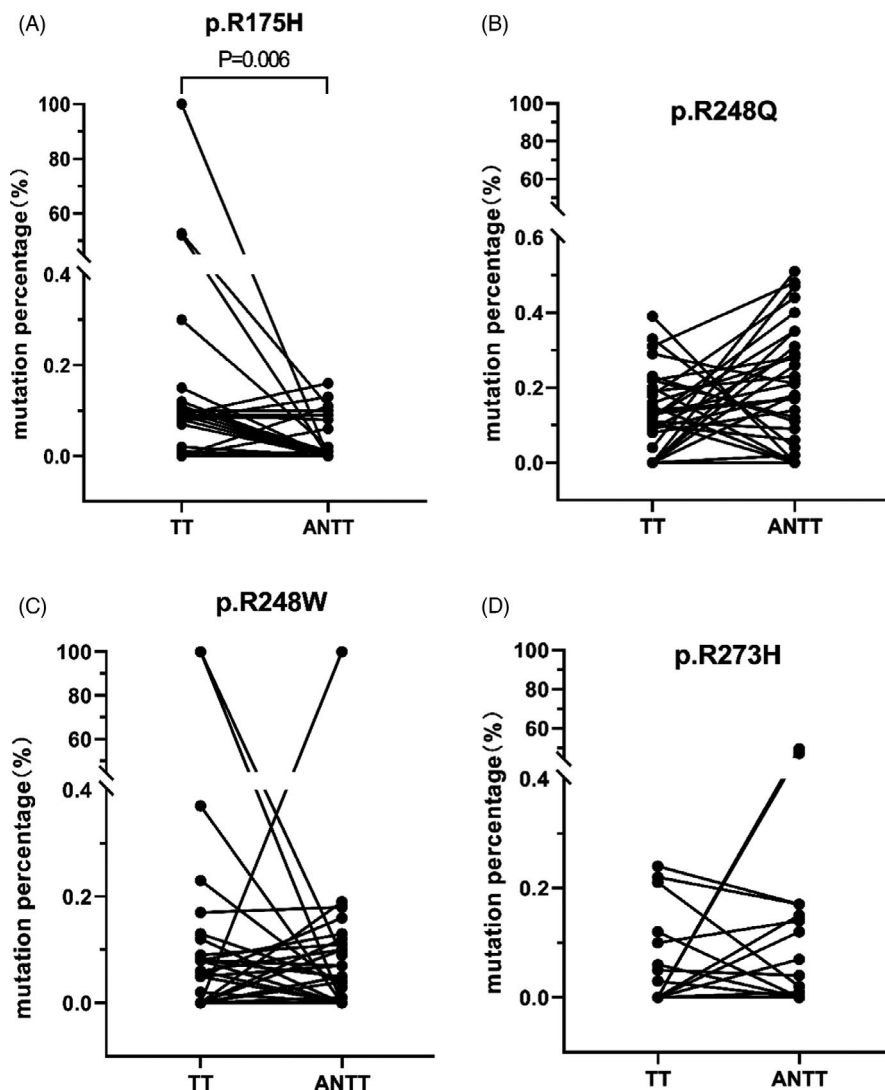
3.4 | Higher p.R273H mutation indicated poor survival of BTC

In this study, BTC patients had a PFS time ranging from 1 to 66 months, with a median survival time of 18 months. Kaplan-Meier curve analysis revealed that the mutant p.R273H patients demonstrated a significantly lower median OS than the wild p.R273H subgroup (median OS: 14.0 vs. 20.0 months, $p = 0.032$, Figure 4D). Similarly, patients with mutant p.R273H showed worse PFS compared to those with wild p.R273H (median PFS: 14.0 vs. 20.0 months, $p = 0.046$, Figure 4E). Due to the limited case of BTC enrolled, no further stratification regarding the quantitative p.R273H and survival was analyzed.

4 | DISCUSSION

BTC is a rare malignancy often identified at an advanced stage and has extremely poor prognoses. The classification of BTC is complex, and the biological characteristics of each subtype are heterogeneous; therefore, the early diagnosis of the disease is full of challenges.²⁰ Most patients are diagnosed at advanced stage when treatment is limited to palliative chemotherapy.²¹ There are limited

FIGURE 2 Comparison of the mutation frequencies of TP53 in TTs and ANTTs. The mutation frequencies of p.R175H, p.R248Q, p.R248W, and p.R273H of TP53 gene from 45 cases of BTC were compared between TTs and ANTTs. Higher mutation of p.R175H occurred in TTs compared with ANTTs ($p = 0.006$). TT, tumor tissue; ANTT, adjacent non-tumor tissue



options regarding systemic therapy for this disease and historically only multi-agent chemotherapy regimens achieve meaningful responses, but the treatment effect is not satisfied.²² At present, effective treatment of BTC is in its pacing stage, while genomic profiling of BTC has gradually becoming a reality which allows a better understanding of its biological characteristics and potential new therapeutic targets.²³

Compared with histopathological tumor tissue analysis, liquid biopsy has already shown more advantages in deciphering a full picture of the patient's genomic, such as overcoming the heterogeneity of the tumor and reducing the disadvantages of the invasive sampling and sample error.²⁴ Digital PCR is one of the most important molecular detection methods in liquid biopsy since dPCR is an accurate nucleic acid quantification method with single-molecule sensitivity. The simplification and visualization of the operation workflow as well as the compatibility of the instrument of ddPCR have greatly accelerated its application in clinical diagnostics.²⁵ DPCR is particularly suitable for monitoring the potential early metastatic recurrence of cancers, low DNA shedding tumors, and rare mutations in complex background especially in circulating tumor DNA (ctDNA).²⁶

CtDNA can be extracted from peripheral blood and has been identified as the ideal detection target helping to reveal the status of gene mutations.²⁷

In our previous study using NGS, we confirmed that the tissue TP53 mutations are the most frequent in BTC, similar to several other types of tumors.²⁸⁻³⁰ Furthermore, our pilot study on searching the hotspot TP53 mutation loci with COSMIC database indicated that p.R175H, p.R248Q, p.R248W, and p.R273H were the four most common mutations of TP53 in BTC using NGS (Table S3). Recently, the research on these loci mainly focused on the pathogenesis indicating that p.R273H can lead to more aggressive phenotypes and enhance cancer cell malignancy, which might be useful in clinical diagnosis and therapy of TP53 mutant cancers.³¹ Some researchers revealed that the mutation TP53-p.R175H was more likely to cause higher levels of genomic instability than the other TP53 mutations.³² Our research in BTC tissues found that the mutation frequency of p.R175H was significantly higher in TT than in ANTT (Figure 2) and the genomic instability of p.R175H might be the possible cause of tumorigenesis and metastasis. Recent studies reported that p53 mutants, including two of the common cancer mutants (R175H and

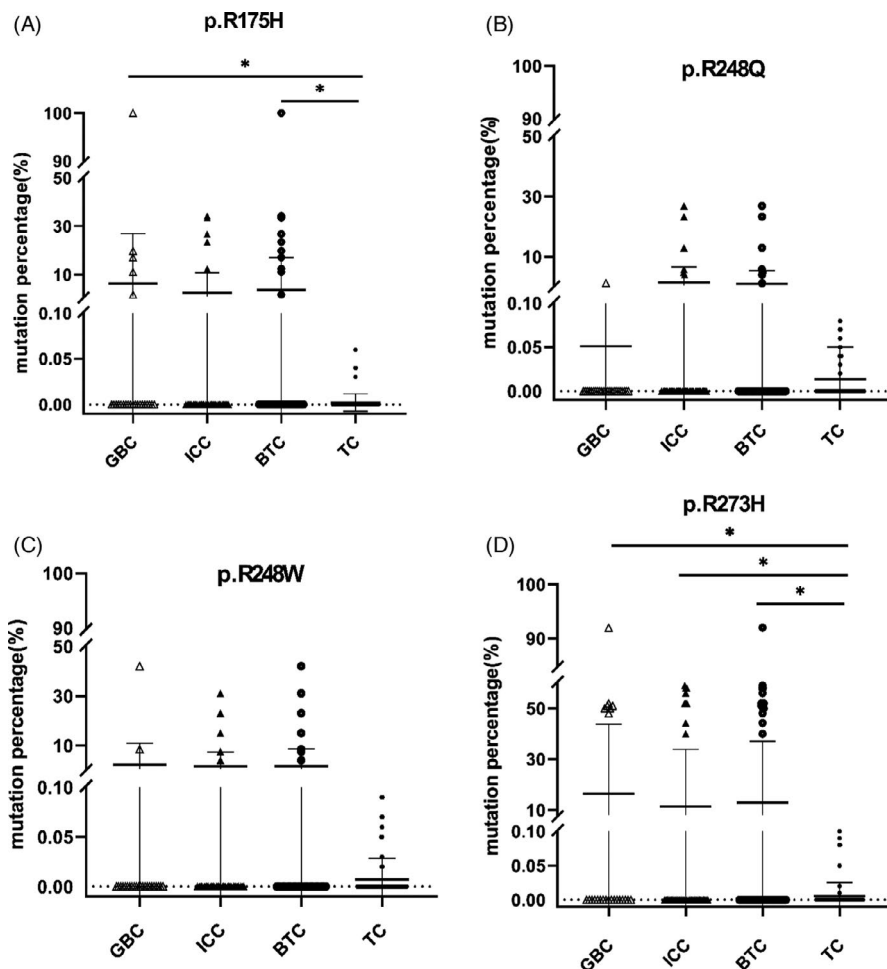


FIGURE 3 Comparison of the TP53 mutation frequencies in cfDNA between BTCs and control groups. Quantitative TP53 mutation detection in plasma cfDNA was measured using ddPCR. TC was used as the control group to compare the differences in mutation frequencies of all four loci (p.R175H, p.R248Q, p.R248W, and p.R273H) of TP53 gene in each experimental group (GBC, ICC, and BTC). The X-axis represents various groups, and the Y-axis represents the mutation frequency of each loci. The mutation frequencies in GBCs and BTCs at p.R175H were higher than that in TC ($p < 0.05$). Meanwhile, the mutation frequencies in different experimental group (GBC, ICC, and BTC) at p.R273H were higher than that in TC ($p < 0.05$). GBC, gallbladder cancer; ICC, intrahepatic cholangiocarcinoma; BTC, biliary tract tumor (GBC + ICC); DC, disease control group; and TC, total control group. The significant differences were marked with * for $p < 0.05$; ** for $p < 0.01$

Mutation loci	ddPCR	TNM stage(n = 76)			Tumor number(n = 76)		
		I-III	IV	p Value	Single	Multiple	p Value
p.R175H	Negative	39	26	0.993	50	15	0.762
	Positive	6	5		8	3	
p.R248Q	Negative	41	28	0.907	55	14	0.086
	Positive	4	3		3	4	
p.R248W	Negative	41	28	0.907	55	14	0.086
	Positive	4	3		3	4	
p.R273H	Negative	36	22	0.363	41	17	0.005*
	Positive	9	9		6	12	

Note: Patients were classified according to the positivity of mutations, and then comparisons were made between negative and positive subgroups on the stages of TNM and the number of tumors. TNM, tumor node metastases. The significant differences were marked with * for $p < 0.05$.

R273H), were more prone to drive the p53 DNA-binding domain toward aggregation-prone conformations than wild type (WT) p53 and these pathological aggregations can lead to diverse cancers.³³ But up to now the researches on these 4 loci are basically limited to the in vitro cellular level and have not been explored clinically, let alone related analysis in diagnosis and prognosis study.

Mounting evidences indicate that the hotspot mutation like p53-R273H promotes cell migration, invasion in vitro, and tumor metastasis in vivo.³⁴ In addition to this pathogenesis of mutant p.R273H,

our experiments had further indicated for the first time that p.R273H might be also useful in clinical diagnosis. In order to make differentiation between BTC and the benign biliary tract disease-calculous cholecystitis, three diagnostic models, Model273-1 for identifying BTC, Model273-2 for GBC, and Model273-3 for ICC, were constructed integrating TP53 mutation and routine tumor maker based on logistic regression. As a result, the logistic algorithm separated BTC from the DC subjects with higher performance than CA19-9, CEA, and AFP did (AUC 0.845 vs 0.786, 0.751 and 0.692, Figure 4). In

TABLE 1 Association between the mutations of TP53 in cfDNA and clinicopathological features

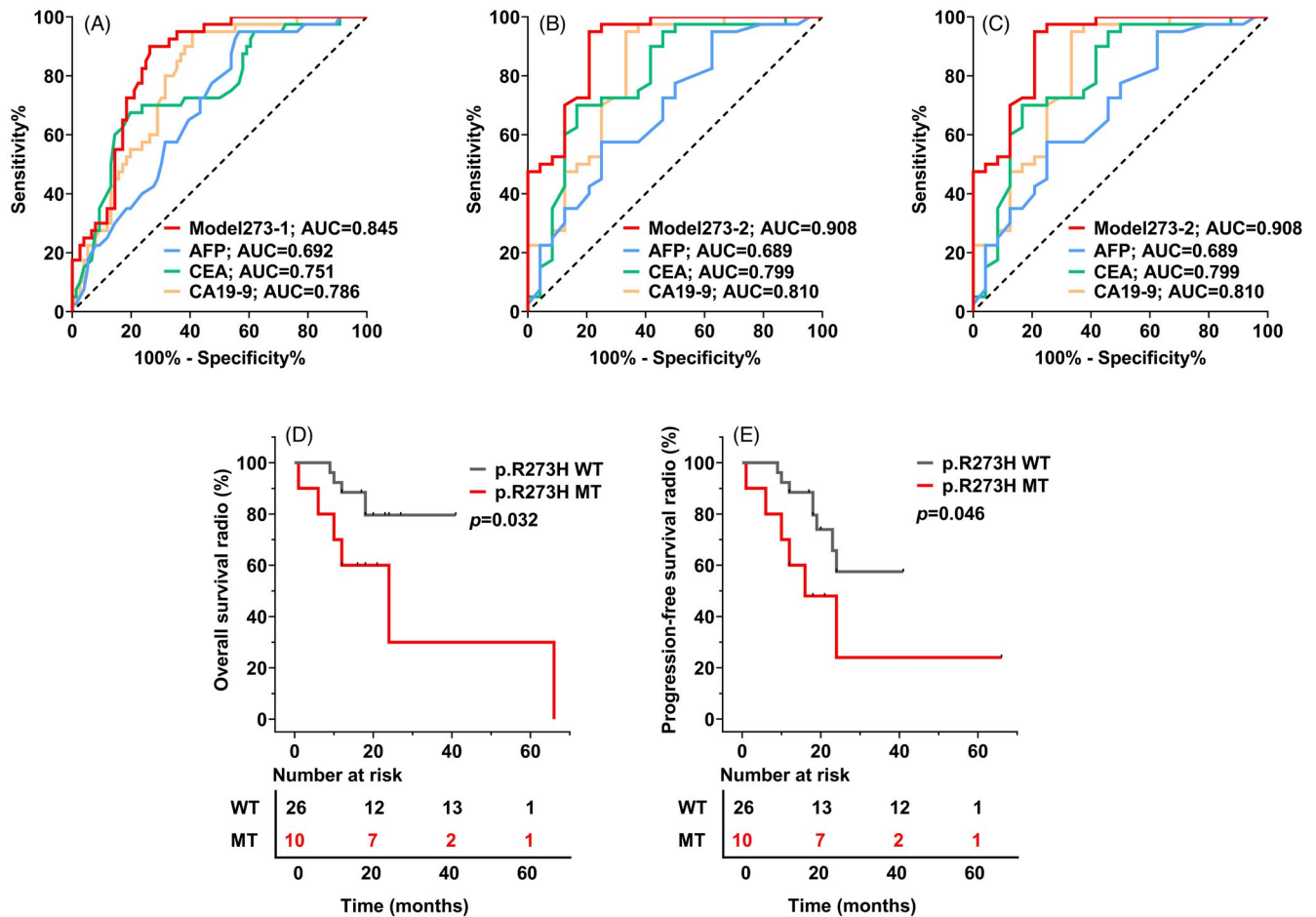


FIGURE 4 Diagnostic performances of three logistic algorithms constructed and the contribution of quantitative p.R273H mutation frequencies to survival outcome in BTC. (A–C) The receiver operating characteristic (ROC) curves of the three p.R273H-based logistic algorithms, CA19-9, CEA, and AFP, indiscriminating different BTCs and the diseases controls (DCs). The area under the ROC curves (AUC) showed the diagnosis powers of the logistic algorithms were better than that of CA19-9, CEA, and AFP in the BTC(A)/GBC(B)/ICC(C) group. (D–E) Kaplan–Meier curves showed that there were significant differences between with (green) and without (gray) p.R273H mutation in the OS and PFS ($p < 0.01$), indicating that BTC patients with p.R273H mutation suffer a poorer prognosis than those without. WT, wild type; MT, mutated type

addition, the diagnostic accuracies of BTC were better than CA19-9, CEA, and AFP (79.31% vs 71.55%, 39.66%, 61.21%). Furthermore, for precise differentiating the subtypes of BTC (GBC and ICC) from the disease controls, the diagnostic accuracies of the novel logistic algorithms (Model273-2/3) were also satisfactory (AUC: 0.908, 95%CI: 0.831–0.985/AUC: 0.844, 95%CI: 0.764–0.924). Moreover, the mutant and wild type of p.R273H could stratify BTC into two distinct subgroups with high or low risks of overall survival and recurrence this noninvasive. Our research helped to accurately reflect intratumoral heterogeneity, assess disease progress, track the trace dynamic gene changes that occurred during follow-up, and help early intervention.

In the present study, TP53 mutations at p.R175H, p.R248Q, p.R248W, and p.R273H were stably detected at a prevalence as low as 0.01% using the QX200 ddPCR system. To evaluate the stability of the quantitation using ddPCR, we used the commercial TP53 p.R175H/p.R273H reference standard to verify the precision of the detection. The results showed that the

within-run coefficient of variation (CV) was 1.2%–11.37% (see Table S4). Furthermore, the between-run CV was 8.87%–9.23% when the standard was diluted into 1% (see Table S5). The liquid biopsy using ddPCR in this study was not affected by the calibration curve, exhibiting decreased variability, superior day-to-day reproducibility, and sensitivity.^{35,36} As recently highlighted, for the ddPCR detection of quantify trace nucleic acids, determining the appropriate threshold is a major issue for reliable results.³⁷ In addition, highly sensitive ddPCR may avoid false-negative results that are associated with tumor heterogeneity in the evaluation of enriched samples in tumor cells.³⁸ With the sensitive and reliable method here, we found some low-frequency (<5%) mutations [p.R175H(8/13), p.R248Q(12/13), p.R248W(5/8), and p.R273H(6/6)] in BTC tissues. Previous studies indicated mutation of TP53 in BTC is 32%–47.1%.^{39,40} Our findings were consistent with previous prevalent viewpoints that the positive mutation rates of these tissue and plasma samples were 51.1% (23/45) and 42.11% (32/76), respectively (see Table S2). The TP53 mutation

TABLE 2 Diagnostic performances of the three p.R273H-based logistic regression models and CA19-9, CEA, and AFP

	Index	AUC (95%CI)	Cutoff value	Sensitivity (%)	Specificity (%)	Accuracy (%)	PPV (%)	NPV (%)
BTC vs DC	Model273-1	0.845 (0.775–0.914)	0.547	73.7	90.0	79.31	93.3	64.3
	CA19-9	0.786 (0.704–0.867)	37.85	59.2	95.0	71.55	95.7	55.1
	CEA	0.751 (0.657–0.845)	1.65	80.3	67.5	39.66	82.4	64.3
	AFP	0.692 (0.596–0.788)	3.45	43.4	95.0	61.21	94.3	46.9
GBC vs DC	Model273-2	0.908 (0.831–0.985)	0.177	79.2	95.0	89.06	90.5	88.4
	CA19-9	0.810 (0.691–0.929)	43.6	66.7	95.0	84.38	88.9	82.6
	CEA	0.799 (0.679–0.919)	1.85	83.3	70.0	75.00	62.5	87.5
	AFP	0.689 (0.553–0.825)	2.45	75.0	57.5	64.06	51.4	79.3
ICC vs DC	Model273-3	0.844 (0.764–0.924)	0.47	75.0	90.0	81.52	90.7	73.5
	CA19-9	0.775 (0.679–0.870)	37.85	55.8	95.0	72.83	93.5	62.3
	CEA	0.729 (0.623–0.836)	1.65	78.8	67.5	73.91	75.9	71.1
	AFP	0.694 (0.587–0.801)	3.45	46.2	95.0	67.39	92.3	57.6

Note: Model273-1/2/3 were logistic algorithms using p.R273H mutation and routine laboratory tests. CA19-9, carbohydrate antigen 19-9; CEA, carcinoembryonic antigen; AFP, alpha-fetoprotein; BTC, biliary tract tumor; GBC, gallbladder cancer; ICC, intrahepatic cholangiocarcinoma; DC, disease control group; AUC, area under curves; CI, confidence interval; PPV, positive predictive value; and NPV, negative predictive value.

rate of our study was higher than those from COSMIC study since low-frequency mutations (<5%) might not be identified by NGS and Sanger sequencing in those studies.

There were some limitations in this study. Firstly, we failed to obtain the matched BTC tissue and plasma cfDNA since this was a retrospective study. Accordingly, we could not evaluate the concordance and difference of TP53 mutations between plasma cfDNA and tissue from the same patients. Secondly, the recruit subjects' number of this study was limited, and the reliability of the models constructed in this study need further independent validation. To overcome the above-mentioned limitations, prospective studies with time-matched blood and tissue samples obtained from more BTC patients are necessary in order to further evaluate the performance of the TP53 mutation-based assessing system developed in this study.

In conclusion, we had shown that dPCR was a simple, noninvasive, and efficient method allowing the detection of TP53 molecular abnormalities in cfDNA. DPCR could help in gaining further insight into the complex landscape of BTC genetic features. In considering the spatial heterogeneity of tumors and the low-frequency mutations detection, our results suggested that mutation of TP53 (p.R273H) detection using dPCR might be a helpful alternative for BTC identification and prognosis prediction. Further studies are required to validate the clinical implications of this TP53 mutation in the management of BTC.

ACKNOWLEDGMENTS

We would like to thank Dr. Xing Gu and Ms. Minfan Xu for their kind assistance in tissue and blood sample collection.

CONFLICT OF INTEREST

All authors claim that there is no conflict of interest including a desire for financial gain, prominence, professional advancement, or a successful outcome.

AUTHOR CONTRIBUTIONS

All authors have accepted responsibility for the entire content of this study and approved its submission.

ETHICAL APPROVAL

The study was approved by the Institutional Review Boards at the leading study center (EHBHKY2020-02-012).

INFORMED CONSENT

Informed consent was obtained from all individuals included in this study.

DATA AVAILABILITY STATEMENT

The datasets generated and/or analyzed during the current study are available from the corresponding author on reasonable request.

ORCID

Xiao Xiao  <https://orcid.org/0000-0002-9260-4519>

Chunfang Gao  <https://orcid.org/0000-0002-4891-2944>

REFERENCES

1. Yang W, Sun Y. Promising molecular targets for the targeted therapy of biliary tract cancers: an overview. *Onco Targets Ther.* 2021;14:1341-1366.
2. Mondaca S, Nervi B, Pinto M, Abou-Alfa GK. Biliary tract cancer prognostic and predictive genomics. *Chin Clin Oncol.* 2019;8:42.
3. Lin HZ, Zhang T, Chen MY, Shen JL. Novel biomarkers for the diagnosis and prognosis of gallbladder cancer. *J Dig Dis.* 2021;22:62-71.
4. Personeni N, Lleo A, Pressiani T, Colapietro F, Openshaw MR, Stavrou C, et al. Biliary tract cancers: molecular heterogeneity and new treatment options. *Cancers.* 2020;12(11):3370.
5. Chae H, Kim D, Yoo C, et al. Therapeutic relevance of targeted sequencing in management of patients with advanced biliary tract cancer: DNA damage repair gene mutations as a predictive biomarker. *Eur J Cancer.* 2019;120:31-39.

6. Marks EI, Yee NS. Molecular genetics and targeted therapeutics in biliary tract carcinoma. *World J Gastroenterol*. 2016;22:1335-1347.
7. Ruiz-Cordero R, Devine WP. Targeted therapy and checkpoint immunotherapy in lung cancer. *Surg Pathol Clin*. 2020;13:17-33.
8. Parris BA, Shaw E, Pang B, Soong R, Fong K, Soo RA. Somatic mutations and immune checkpoint biomarkers. *Respirology*. 2019;24:215-226.
9. de Melo-Silva AJ, Lucena JP, Hueneburg T. The evolution of molecular diagnosis using digital polymerase chain reaction to detect cancer via cell-free DNA and circulating tumor cells. *Cell Biol Int*. 2020;44:735-743.
10. Sato Y, Matoba R, Kato K. Recent advances in liquid biopsy in precision oncology research. *Biol Pharm Bull*. 2019;42:337-342.
11. Raso A, Biassoni R. A Quarter century of PCR-applied techniques and their still-increasing fields of use. *Methods Mol Biol*. 2020;2065:1-4.
12. Cao L, Cui X, Hu J, et al. Advances in digital polymerase chain reaction (dPCR) and its emerging biomedical applications. *Biosens Bioelectron*. 2017;90:459-474.
13. Quan PL, Sauzade M, Brouzes E. dPCR: A Technology Review. *Sensors*. 2018;18:1271.
14. Suo T, Liu X, Feng J, et al. ddPCR: a more accurate tool for SARS-CoV-2 detection in low viral load specimens. *Emerg Microbes Infect*. 2020;9:1259-1268.
15. Coccaro N, Tota G, Anelli L, Zagaria A, Specchia G, Albano F. Digital PCR: a reliable tool for analyzing and monitoring hematologic malignancies. *Int J Mol Sci*. 2020;21.
16. Mahendran P, Liew JWK, Amir A, Ching XT, Lau YL. Droplet digital polymerase chain reaction (ddPCR) for the detection of *Plasmodium knowlesi* and *Plasmodium vivax*. *Malar J*. 2020;19:241.
17. Yamamoto S, Iwakuma T. Regulators of oncogenic mutant TP53 gain of function. *Cancers (Basel)*. 2018;11:4.
18. Xu F, Lin H, He P, et al. A TP53-associated gene signature for prediction of prognosis and therapeutic responses in lung squamous cell carcinoma. *Oncoimmunology*. 2020;9:1731943.
19. Feng F, Wu X, Shi X, et al. Comprehensive analysis of genomic alterations of Chinese hilar cholangiocarcinoma patients. *Int J Clin Oncol*. 2021;26:717-727.
20. Nara S, Esaki M, Ban D, et al. Adjuvant and neoadjuvant therapy for biliary tract cancer: a review of clinical trials. *Jpn J Clin Oncol*. 2020;50:1353-1363.
21. Lamarca A, Barriuso J, McNamara MG, Valle JW. Biliary tract cancer: state of the art and potential role of DNA damage repair. *Cancer Treat Rev*. 2018;70:168-177.
22. Jakubowski CD, Azad NS. Immune checkpoint inhibitor therapy in biliary tract cancer (cholangiocarcinoma). *Chin Clin Oncol*. 2020;9:2.
23. Morizane C, Ueno M, Ikeda M, Okusaka T, Ishii H, Furuse J. New developments in systemic therapy for advanced biliary tract cancer. *Jpn J Clin Oncol*. 2018;48:703-711.
24. Russano M, Napolitano A, Ribelli G, et al. Liquid biopsy and tumor heterogeneity in metastatic solid tumors: the potentiality of blood samples. *J Exp Clin Cancer Res*. 2020;39:95.
25. Xu L, Qu H, Alonso DG, et al. Portable integrated digital PCR system for the point-of-care quantification of BK virus from urine samples. *Biosens Bioelectron*. 2021;175:112908.
26. Guibert N, Pradines A, Farella M, et al. Monitoring KRAS mutations in circulating DNA and tumor cells using digital droplet PCR during treatment of KRAS-mutated lung adenocarcinoma. *Lung Cancer*. 2016;100:1-4.
27. Chapman L, Ledet EM, Barata PC, et al. TP53 gain-of-function mutations in circulating tumor DNA in men with metastatic castration-resistant prostate cancer. *Clin Genitourin Cancer*. 2020;18:148-154.
28. Wardell CP, Fujita M, Yamada T, et al. Genomic characterization of biliary tract cancers identifies driver genes and predisposing mutations. *J Hepatol*. 2018;68:959-969.
29. Yang P, Javle M, Pang F, et al. Somatic genetic aberrations in gallbladder cancer: comparison between Chinese and US patients. *Hepatobiliary Surg Nutr*. 2019;8:604-614.
30. Roos E, Soer EC, Klompaker S, et al. Crossing borders: A systematic review with quantitative analysis of genetic mutations of carcinomas of the biliary tract. *Crit Rev Oncol Hematol*. 2019;140:8-16.
31. Kang N, Wang Y, Guo S, et al. Mutant TP53 G245C and R273H promote cellular malignancy in esophageal squamous cell carcinoma. *BMC Cell Biol*. 2018;19:16.
32. Samassekou O, Bastien N, Lichtensztejn D, Yan J, Mai S, Drouin R. Different TP53 mutations are associated with specific chromosomal rearrangements, telomere length changes, and remodeling of the nuclear architecture of telomeres. *Genes Chromosomes Cancer*. 2014;53:934-950.
33. Li L, Li X, Tang Y, Lao Z, Lei J, Wei G. Common cancer mutations R175H and R273H drive the p53 DNA-binding domain towards aggregation-prone conformations. *Phys Chem Chem Phys*. 2020;22:9225-9232.
34. Lv T, Wu X, Sun L, et al. p53-R273H upregulates neuropilin-2 to promote cell mobility and tumor metastasis. *Cell Death Dis*. 2017;8:e2995.
35. Hindson CM, Chevillet JR, Briggs HA, et al. Absolute quantification by droplet digital PCR versus analog real-time PCR. *Nat Methods*. 2013;10:1003-1005.
36. Bosman KJ, Nijhuis M, van Ham PM, et al. Comparison of digital PCR platforms and semi-nested qPCR as a tool to determine the size of the HIV reservoir. *Sci Rep*. 2015;5:13811.
37. Thierry AR, Mouliere F, El Messaoudi S, et al. Clinical validation of the detection of KRAS and BRAF mutations from circulating tumor DNA. *Nat Med*. 2014;20:430-435.
38. Jiang XW, Liu W, Zhu XY, Xu XX. Evaluation of EGFR mutations in NSCLC with highly sensitive droplet digital PCR assays. *Mol Med Rep*. 2019;20:593-603.
39. Wu CE, Pan YR, Yeh CN, Lunec J. Targeting P53 as a future strategy to overcome gemcitabine resistance in biliary tract cancers. *Biomolecules*. 2020;10:1474.
40. Li M, Zhang Z, Li X, et al. Whole-exome and targeted gene sequencing of gallbladder carcinoma identifies recurrent mutations in the ErbB pathway. *Nat Genet*. 2014;46:872-876.

SUPPORTING INFORMATION

Additional supporting information may be found in the online version of the article at the publisher's website.

How to cite this article: Xiao X, Zhou J, Fang M, et al. Quantitative detections of TP53 gene mutations improve the diagnosis and prognostic prediction of biliary tract cancers using droplet digital PCR. *J Clin Lab Anal*. 2022;36:e24103. <https://doi.org/10.1002/jcla.24103>